AD-A153 650 MICRO-REACTIONS OF METAL CONTACTS ON VARIOUS TYPES OF GAAS SURFACES(U) TECHNISCHE HOCHSCHULE DARMSTADT (GERMANY F R) INST FUER HOCHF.. H L HARTNAGEL ET AL. 1/1

UNCLASSIFIED JAN 85 DAJA45-83-C-0012 F/G 7/4 NL

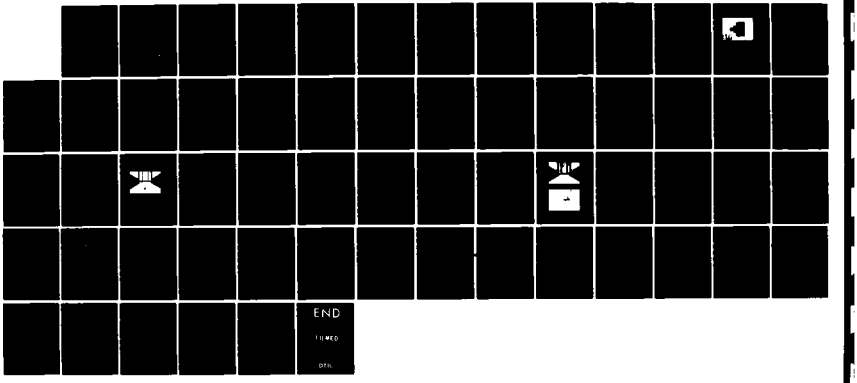

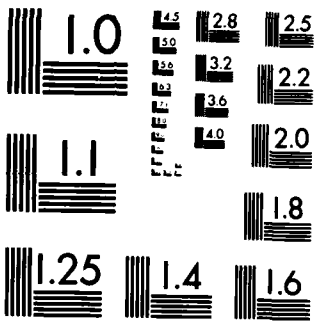

MICROCOPY RESOLUTION TEST CHART
NATIONAL BUREAU OF STANDARDS-1963-A

Institut für Hochfrequenztechnik
Technische Hochschule
Darmstadt

MICRO-REACTIONS OF METAL CONTACTS ON VARIOUS TYPES OF GaAs SURFACES

2nd Annual Technical Report

H.L. Hartnagel [+]

K.-H. Kretschmer

B. R. Sethi

J. Würfl

J A N U A R Y 1985

European Research Office
United States Army
London NW 1 5TH, England

GRANT NUMBER DAJA 45-83-C-0012

Technische Hochschule Darmstadt
Institut für Hochfrequenztechnik
Merckstraße 25, 6100 Darmstadt / FRG

[+]Grant Holder

SECURITY CLASSIFICATION OF THIS PAGE (When Data Entered)

REPORT DOCUMENTATION PAGE

READ INSTRUCTIONS BEFORE COMPLETING FORM

1. REPORT NUMBER	2. GOVT ACCESSION NO. / 3. RECIPIENT'S CATALOG NUMBER
4. TITLE (and Subtitle): Micro-Reactions of Metal Contacts on Various Type of GaAs Surfaces	5. TYPE OF REPORT & PERIOD COVERED: 2nd Annual Technical Report January 1984-January 1985
	6. PERFORMING ORG. REPORT NUMBER
7. AUTHOR(s): H.L. Hartnagel, K.-H. Kretschmer, B.R. Sethi, J. Würfl	8. CONTRACT OR GRANT NUMBER(s): DAJA 45-83-C-0012
9. PERFORMING ORGANIZATION NAME AND ADDRESS: Institut für Hochfrequenztechnik, Technische Hochschule Darmstadt, Merckstr. 25, 6100 Darmstadt, G.F.R.	10. PROGRAM ELEMENT, PROJECT, TASK AREA & WORK UNIT NUMBERS
11. CONTROLLING OFFICE NAME AND ADDRESS	12. REPORT DATE: January 1985
	13. NUMBER OF PAGES: 57
14. MONITORING AGENCY NAME & ADDRESS (if different from Controlling Office)	15. SECURITY CLASS. (of this report)
	15a. DECLASSIFICATION/DOWNGRADING SCHEDULE

16. DISTRIBUTION STATEMENT (of this Report)

17. DISTRIBUTION STATEMENT (of the abstract entered in Block 20, if different from Report)

18. SUPPLEMENTARY NOTES

19. KEY WORDS (Continue on reverse side if necessary and identify by block number)

GaAs, Metallization Stability, XPS, ISS, GaAs surface chemistry.

20. ABSTRACT (Continue on reverse side if necessary and identify by block number)

Further XPS analysis results of a range of GaAs surfaces are reported which are produced by various technological steps such as etching in basic or acidic solutions as customary before the deposition of metals. The findings of lateral material transport between co-planar electrodes, on Metal-GaAs interdiffusion due to typical operational device conditions and on the "electron wind" in narrow conductors are presented.

DD FORM 1 JAN 73 1473 EDITION OF 1 NOV 65 IS OBSOLETE

SECURITY CLASSIFICATION OF THIS PAGE (When Data Entered)

TABLE OF CONTENTS

ABSTRACT

Further XPS analysis results of a range of GaAs surfaces are reported which are produced by various technological steps such as etching in basic or acidic solutions as costumary before the deposition of metals.
The findings of lateral material transport between co-planar electrodes, across metal-GaAs junctions and in narrow conductors, all due to the application of high fields or currents, are presented as to be found under operational conditions of devices such as MESFETs.

List of Keywords

GaAs, metallization stability, XPS, ISS, GaAs surface chemistry.

CHAPTER I

INTRODUCTION

GaAs-metal contacts form an important part of microwave and optical devices, and their stability is essential for the desired long life-times. It is therefore necessary to study life-time effects of metal contacts on the various technology-type surfaces when GaAs surfaces are not ideal as produced by cleavage under ultra-high vacuum. The different semiconductor surfaces are indeed found to cause strongly varying behaviour concerning such life-time effects as field-assisted diffusion of metal along GaAs, or interdiffusion across the metal-semiconductor transition. The investigations described in this report therefore do not cover the phenomena associated with clean ideal surfaces. Neither, do we study directly life-time effects on devices, as for example reported by various industrial laboratories (for example |1|).

We address our efforts towards a more fundamental study of the physics and chemistry of interactions associated with metals on GaAs surfaces as found with practical devices. Therefore, initially an investigation was undertaken to evaluate the conditions of the GaAs surfaces as found after all the typical technology steps of device manufacture are applied such as sputter etching, rinsing in water, exposure to air, etching in common etchants etc. (see First Annual Report). This has resulted in a large number of new, sometimes unexpected results relevant for an

understanding of the various phenomena observed by device-fabrication technologists. In the second part of our program, the study of the stability of metal films on these GaAs surfaces was undertaken under typical device-operational conditions such as high currents or high voltages. Here, interesting, new information can be reported now. However, more work is required to clarify all the related phenomena of device life-time optimization.

CHAPTER II

LATERAL MATERIAL MIGRATION STUDIES

Introduction:

In our last Annual Reports the physical mechanism for field induced material migration was discussed. It was suggested that the applied electric field deforms the surface potential function so that field-assisted diffusion of material along the surfaces causes material migration. It was shown also experimentally that sputtered electrode material enhances material migration and that the type of treatment of the GaAs surface affects the processes strongly.

Therefore, further XPS (X-Ray Photoelectron Spectroscopy) studies of (100)-GaAs surfaces were undertaken now and were correlated with a treshold voltage for material migration. This treshold voltage is defined as the value required for the onset of a practically instantaneous complete short circuiting of neighbouring electrodes (usually within a fraction of a second). In addition to the results presented in our previous Annual Report, some other surface conditions based on a specific selection of etching and cleaning processes as commonly employed for the manufacture of GaAs devices have now been investigated. The XPS-spectra gave detailed information on the type of surface, (e.g. of the layer very close to the surface, of deeper-lying layers, of the absorbed oxygen etc.) which is also of interest concerning the other degradation mechanisms in MeSFETs as presented in subsequent chapters. Concerning related publications, we refer to |1,2|.

Our measured treshold values show that the lateral material migration is indeed strongly influenced by the surface oxygen content.

FABRICATION AND EXPERIMENTAL PROCEDURE

Closely spaced electrode gaps with 2o and 4o μm distances were manufactured to study the field induced material migration. Semiinsulating (s.i.), Cr-doped bulk GaAs with a high resistivity ($>10^8\ \Omega \cdot cm$) was chosen as the substrate so that current-induced heating of the sample does not have to be taken into consideration. After wet-organic cleaning of the substrate, the surfaces were etched for 1 minute with various etching solutions (see Table 1). The first group of samples was treated by a sulfurious acid solution which we commonly employ for mesa-etching. The second group of samples was only cleaned by organic solvents. A pre-evaporation etch was applied to the third group. We found high treshold voltages for the fourth and fifth types, which are basic etchants. The temperature of all etch solutions was 23^0 C. In all cases subsequent rinsing in H_2O and drying in N_2 gas was applied. Then closely-spaced Al-electrode structures were defined by lift-off technique on the differently treated (1oo)-GaAs-surfaces. Fig.1 shows the optical mask with the two closely spaced pairs of electrodes.

The free areas on the test chips, which experienced of course the same treatments as the GaAs-surfaces between the electrodes, were then XPS-analyzed to characterize the resulting surface conditions.

Table 1 : Types of surface treatment

no.	solution	remarks
1	H_2SO_3 (conz.) : H_2O_2 (30 %) : H_2O 1 : 10 : 10	Mesa - Etch
2	only cleaning by organic solvents	
3	NaOH (2%) : H_2O_2 (30 %) (4 Vol %) 1 : 1	Pre-Evaporation - Etch
4	NaOH : H_2O 1 : 5	Etchants with expected higher threshold voltages for material migration
5	KOH : H_2O 5 : 1	

Etch time : 1 minute
Temperature : 23°C

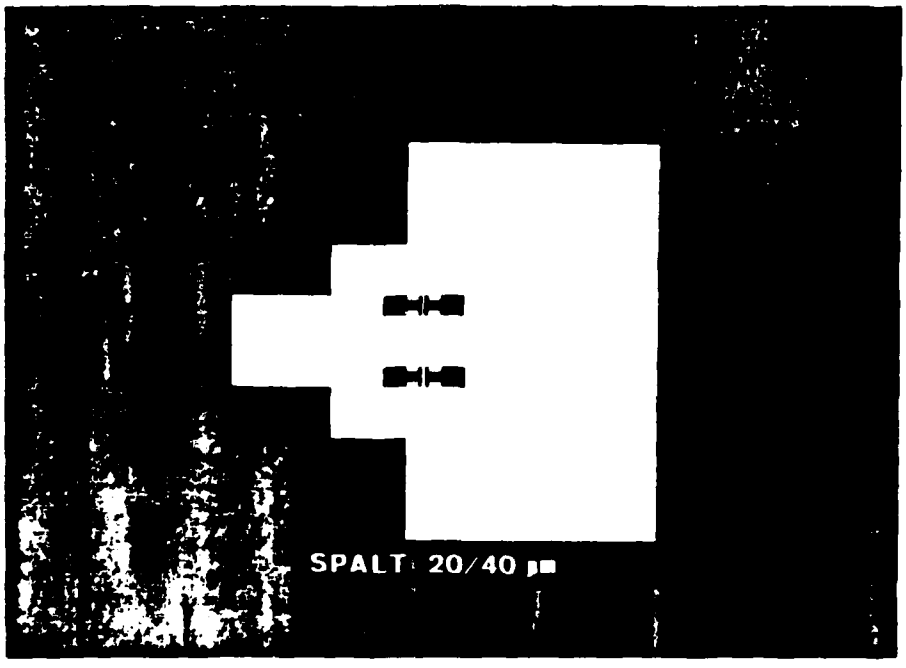

Fig. 1 Photomask of 20 and 40 µm gaps

These measurements were undertaken in a Leybold-Heraeus system with Al K_α radiation (radiation energy: 1486,6 eV). The electron energies were measured by a variable retarding potential and a spherical sector analyser using constant transmission energy which gives constant bandwidths and detection probability for the transmitted electrons.

Accelerated material migration could be observed when applying high voltages between the neighbouring electrodes. The treshold voltage, required for practically instanteneous complete short circuiting of the electrodes by material migration, were measured during standard conditions of 23^{o} C room-temperature and a relative humidity of approximate 65 %.

XPS-ANALYSIS

In connection with the characterization of the differently prepared GaAs samples, the XPS-spectra of As $2p_{3/2}$, Ga $2p_{3/2}$, O 1 s, As 3d and Ga 3d surface electrons were employed. Fig. 2 shows these spectra. They are arranged in accordance with the type of surface treatment by rows 1 to 5. The $2p_{3/2}$ core level emissions of As and Ga are presented in the first two columns. Since the mean free path for the electrons in GaAs without energy loss is energy dependent, the electrons of those lines originate very closely to the surface, typically at a depth of 8 - 12 Å [3]. On the other hand, the 3d, XPS lines of As and Ga originate from the 3d electrons of deeper lying atomic layers with an average depth

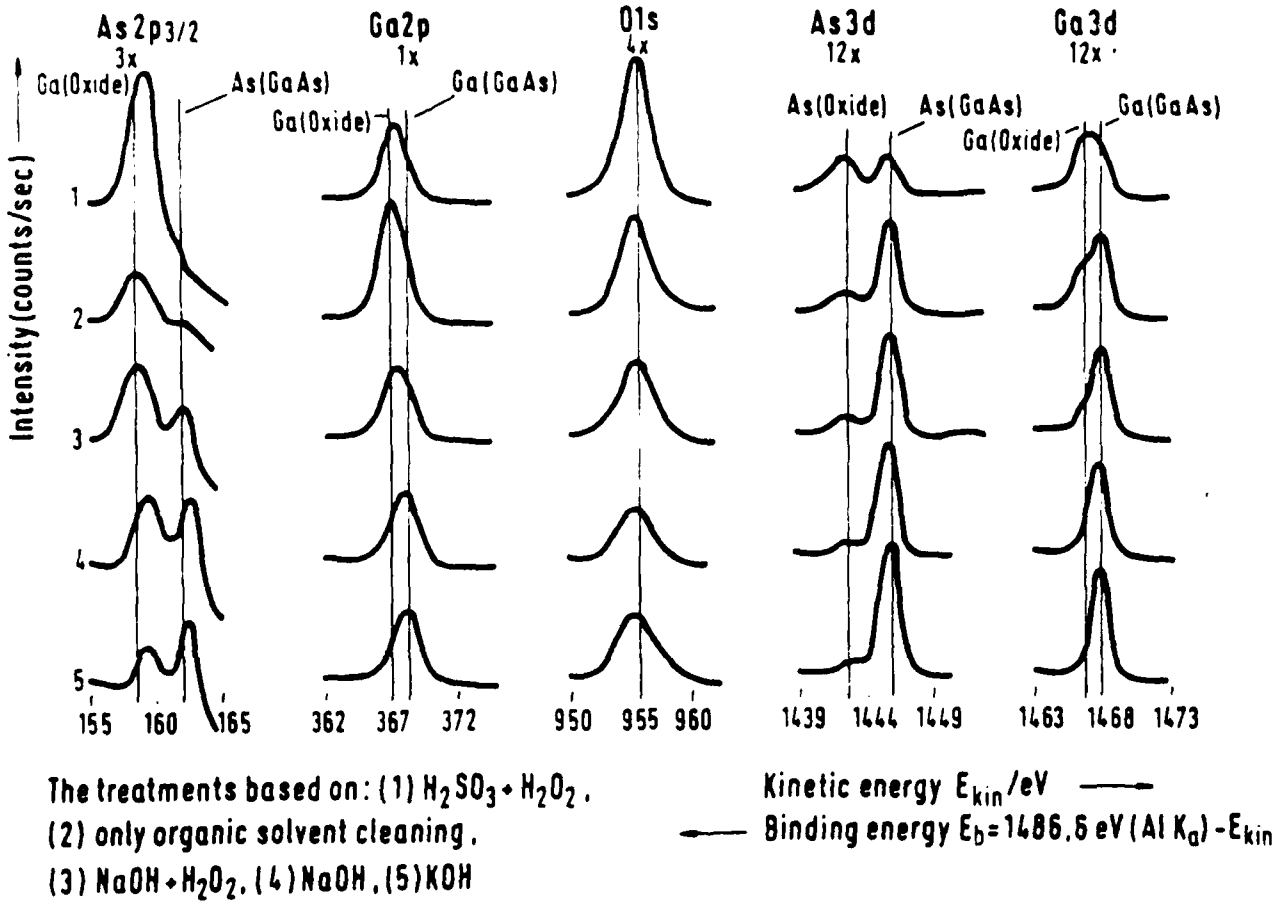

Fig. 2 XPS-spectra of differently treated (100)-GaAs-surfaces

of 25 Å. The 3d core level emissions are given in the two last columns. Additionally the 1s XPS line of oxygen is presented.

In connection with the $2p_{3/2}$ and 3d lines, two separate levels can be distinguished. The levels, representing higher kinetic energies (lower binding energies) originate from those As and Ga atoms which are essentially bonded in connection with the semiconductor GaAs. The level with lower kinetic energies (higher binding energies) are caused by the oxidised forms of As and Ga [4]. The intensity of the maxima with respect to the background noise is a measure of the concentration of the corresponding type of atom.

Using these XPS measurements, the following details can be derived (Fig. 2):

- The non-etched (1oo) GaAs surfaces (row 2) exhibit primarily Ga and As oxides. At increased depth the As oxide is reduced rather quickly to As as bonded to Ga. On the other hand the Ga 3d line demonstrates that its oxide penetrates rather more deeply into the bulk material. This is in agreement with [5] where it was established that As_2O_3 in contact with GaAs should react according to the equation

$$As_2O_3 + 2\ GaAs \longrightarrow Ga_2O_3 + 4\ As$$

yielding Ga_2O_3 and As as the stable phases which can coexist at equilibrium with GaAs.

- When the surfaces are etched in the sulfurious acid solutions (row 1) they exhibit a strong contribution of As oxide. Even down to a depth of about 25 Å such a strong As oxide component ist still present (see the As 3d spectrum).

- Following through the three basic solutions NaOH + H_2O_2, NaOH and KOH (rows 3,4 and 5) both, the As and Ga oxides are removed with increasing extent. The As $2p_{3/2}$ spectra show this particularly clearly by the transfer of intensity to the As which is bonded to Ga. Similarly the Ga $2p_{3/2}$ spectra show this by the shift of the maximum towards the Ga bonded to As. Even at a depth of 25 Å this feature can still be clearly recognized with the Ga 3d line.

DISCUSSION OF RESULTS

Material migration from the anode to the cathode could be observed after the application of high voltages to the neighbouring electrode gaps. The treshold voltages required for quasi-instantaneous complete short circuiting of the electrodes by material migration are given in Table 2. It is obviously that great differences exist depending on the GaAs surface conditions as produced by the various treatment processes.

Table 2 : Dependence of threshold voltage on surface treatment

no.	solution	threshold voltage(typical) 20µm gap	40µm gap
1	H_2SO_3(conz.) : H_2O_2(30%) : H_2O 1 : 10 : 10	50V	90V
2	only cleaning by organic solvents	100V	200V
3	NaOH(2%) : H_2O(30%)(4Vol%) 1 : 1	150V	270V
4	NaOH : H_2O 1 : 5	160V	300V
5	KOH : H_2O 5 : 1	175V	320V

Temperature : 23°C
Rel. humidity : 65%

Samples where the GaAs surface were etched with H_2SO_3 + H_2O_2 showed by 50 % a reduced treshold voltage as compared to the non-etched surfaces, whereas the treshold values for the samples treated by the basic etchants were by 35 % higher than those of non-etched surfaces.

If one compares the XPS measurements with the measured treshold voltages for material migration, one can see that the migration depends very strongly on the amount of As_2O_3 on the surface. Fig. 3 shows the correlation of the treshold voltage with the logarithm of the XPS-ratio of As bonded to oxide to As bonded to GaAs. The agreement of the reduction of the oxygen component with the increase in treshold voltage is surprisingly clear. Whereas the treatments based on alkaline etchants leave a low arsenic oxide to GaAs-ratio with corresponding high treshold values for material migration, the empoloyed acid etch solutions lead to a strongly increased oxide component in the surface with unacceptably low treshold voltages.

Very recently, the "gate-recess" etchant NH_4OH (25 %) : H_2O_2 (30 %) : H_2O of the ratio 2 : 1 : 300 has been investigated, which shows the same good behaviour as the KOH etchant.

In summary, we have reported that electric-field induced migration of electrode material along (100)-GaAs-surfaces strongly depends on surface treatment. A direct correlation between "XPS-GaAs-surface quality"

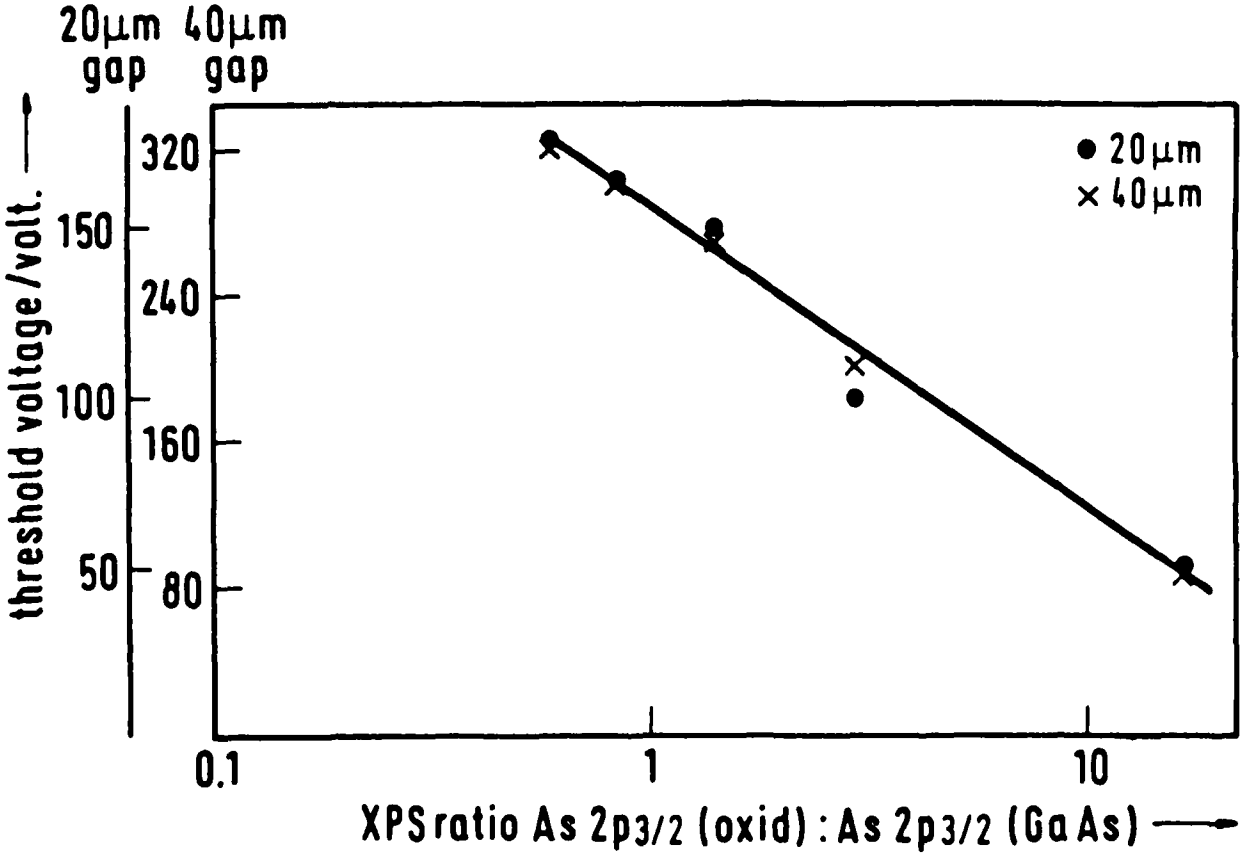

Fig. 3 Threshold voltage for material migration versus XPS-ratio As $2p_{3/2}$ (oxide) : As $2p_{3/2}$ (GaAs)

and interelectrode material has been observed. The XPS-spectra shows:

1. Samples cleaned by organic solvents only, exhibit primarily Ga- and As-oxides.

2. Gallium oxide penetrates more deeply into the bulk material.

3. Surfaces treated by the acid etchant $H_2SO_3 + H_2O_2$ exhibit a strong contribution of arsenic oxide even down to the depth of the order of 25 Å. A reduction of treshold voltage up to 5o % have been observed.

4. The treatment with basic etchants removes both As- and Ga-oxides and hence results in an approximately stoichiometric Ga to As ratio. The treshold voltages are more than 35 % higher than the values for the non-etched surfaces. Best results were obtained for the etchants KOH and $NH_4OH + H_2O_2$.

Using thi, analysis one can conclude that it is necessary to provide as far as possible native-oxide free surfaces between closely-spaced neighbouring electrodes. Since GaAs-surfaces, which are only cleaned by organic solvents, exhibit a high oxygen content, it is desirable to use a suitable surface treatment to achieve a high reliability of GaAs planar devices.

We have now started investigations on other metallisation materials like the ohmic contact composition Au-Ge. To realize some manufacture procedure like in GaAs-MESFET-technology the Au-Ge contacts have to be annealed after deposition. Our first experiments show that this annealing process (usually for 1o sec at 46o^{o} C) changes the surface condition drastically , although the annealing time is very short. The effects on material migration due to the originated surfaces will be taken into consideration by our further investigations.

CHAPTER III

ELECTRON WIND VOIDING IN NARROW METALLIZATIONS AND ITS CHARACTERIZATION WITH PARTICULAR RELEVANCE FOR GaAs MeSFET GATES

Aluminium (Al) is quite commonly used for the Schottky-barrier gate metallization in GaAs MeSFETs [6,7] and also as narrow conductors for biasing and interconnect line in GaAs IC's. When such narrow conducting lines are current stressed (above certain treshold current densities of around $J_{th} \sim 10^5$ A/cm^2), the metal ions under the impact of the electron-wind force (as a result of momentum exchange with the electrons) are dragged along the direction of the electron-flow resulting in electro migration of the material. This mass transport under high current densities is an electron-wind assisted diffusion phenomenon through the grain-boundaries of the metallization under the normal operating conditions of the GaAs device and is characterized by an activation energy E_a, relevant for the existing diffusion mechanism. When the device is under operation, conditions such as temperature gradients, compositional inhomogeneities and particularly the structural variations, e.g. change in grain-size or in grain orientation, give rise to divergencies of ion-flux leading to the formation of vacancies or holes which grow into stable voids as a result of a depletion of material and hillocks and whiskers due to accumulation of material. The growth of the voids results in degradation of the device characteristics and the eventual crack propagation may also lead to a catastrophic failure of the open-circuit type (burn-out) due to electro migration. Therefore, it was decided to investigate the electo migration damage due to the electron-wind effect in Al-metallizations as used for GaAs MeSFETs and for biasing and interconnect lines in their monolothic circuits.

As a first approach, Al-films were evaporated onto Corning glass with and without a chromium-layer interface. The reasons for choosing a Cr-layer underneath the Al-metallization are the following:

- GaAs MeSFET devices are often fabricated on Cr-doped semi-insulating GaAs; Cr has the tendency to accumulate at the surface during operation,
- Cr is used sometimes as a barrier layer in low resistance contacts in GaAs devices and
- Cr is quite often employed as a sticking agent for Al-lines on GaAs

Damage appearing in Al-metallizations due to electron-wind voiding is characterized in terms of the activation energy E_A for electro migration for the relevant diffusion process involved in material migration along with a constant K which depends on the Diffusion coefficient D_o (at $T \to \infty$) on geometric factors and on certain other properties of the metallization, or in terms of the drift velocity v_β of the Al-ions drifting along the grain-boundaries at a particular temperature for a constant current density. The migration of the Al-ions under current density J is related to the activation energy E_A and the const. K through the Arrhenius temperature dependance for D by the basic relation |8|.

$$\frac{v_\beta T}{J} = K \exp\left(-Eg/_{kT}\right) \qquad \text{— (1 a)}$$

$$\text{or } \ln \frac{v_\beta T}{J} = \ln K - \frac{Eg}{k} \cdot \frac{I}{T} \qquad \text{— (1 b)}$$

$$\text{where } K = \frac{D_o\, ez^+\, \rho}{k} \qquad \text{— (1 c)}$$

Eg = the grain-boundary diffusion activation energy
z^+e = the effective equivalent charge on the migrating Al-ion
ρ = the resistivity and k is the Boltzmann constant.

The investigations were performed using two techniques:
1) The meantime to failure (MTF) technique |9|and
2) The Resistometric or Resistance Monitoring (RM) technique

The purpose of performing measurements on a glass substrate was two fold

- to standardise the technique of measurement
- to compare the results obtained with those in Al-metallizations on a GaAs substrate.

After the initial standardisation work, we concluded that the RM technique is more reliable and sensitive for the characterization of the electro migration damage parameters.

Investigations were subsequently performed in Al-metallizations evaporated on a high resistivity GaAs substrate (undoped, surface (100) oriented) with and without the chromium-interface layer, using the RM technique.
For the investigations by the MTF technique, Al-thin film structures of the geometry shown in Fig. 4, with conducting line dimensions width - 10 μm, length - 1oo μm and thickness -1ooo Å were produced by the standard photolithography and electron-beam evaporation from an Al-wire in a vacuum of 1×10^{-6} Torr. Leads were bonded to the wider Al-electrodes (bonding-pads) at the two ends of the conducting line (as shown in Fig. 4) with silver epoxy glue (consisting of parts A and B of H 2o E (mixed with the ration 1 : 1) supplied by Polytec, West-Germany). MTF investigations were performed on these structures for current densities J from 1 to 3×10^6 A/cm^2. Strong electro migration effects were seen even at room temperature over a period of 16 hours for $J = 2 \cdot 5 \times 10^6$ A/cm^2. Material migration was confirmed by observation of the current-stressed line under the optical microscope with a magnification x625, when fine voids or pin-holes were seen on the conducting line at the end near the cathode electrode. Further passage of the current for a longer period resulted in a growth of the voids near the cathode end with a crack developed in 3o hrs across the entire cross-section of the line leading to a catastrophic failure. Examination under the microscope revealed not only cracks near the cathode end, but also some hillocks of migrated Al on the half side of the strip towards the anode electrode along with a number of fine holes near the middle of the conducting line (Fig. 5)

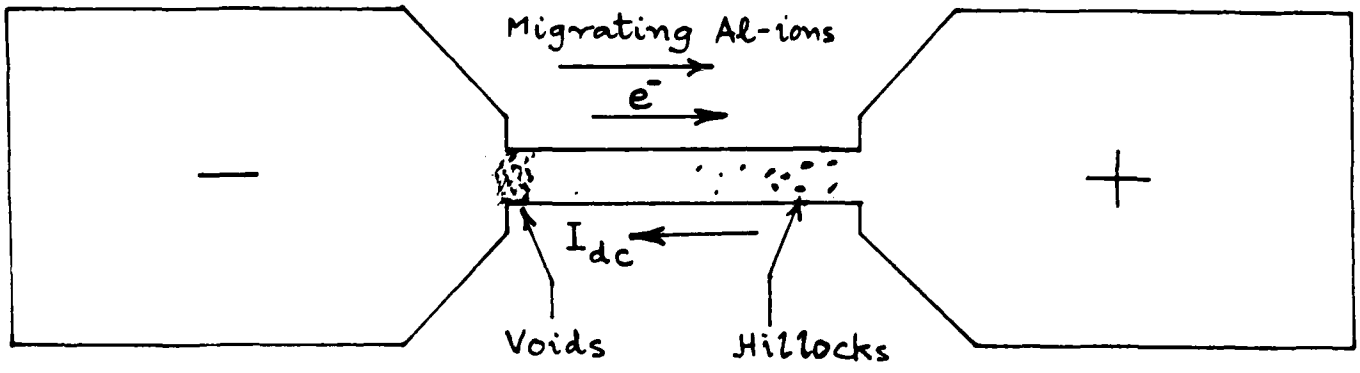

Fig.4 Electromigration at non-uniformities of current densities

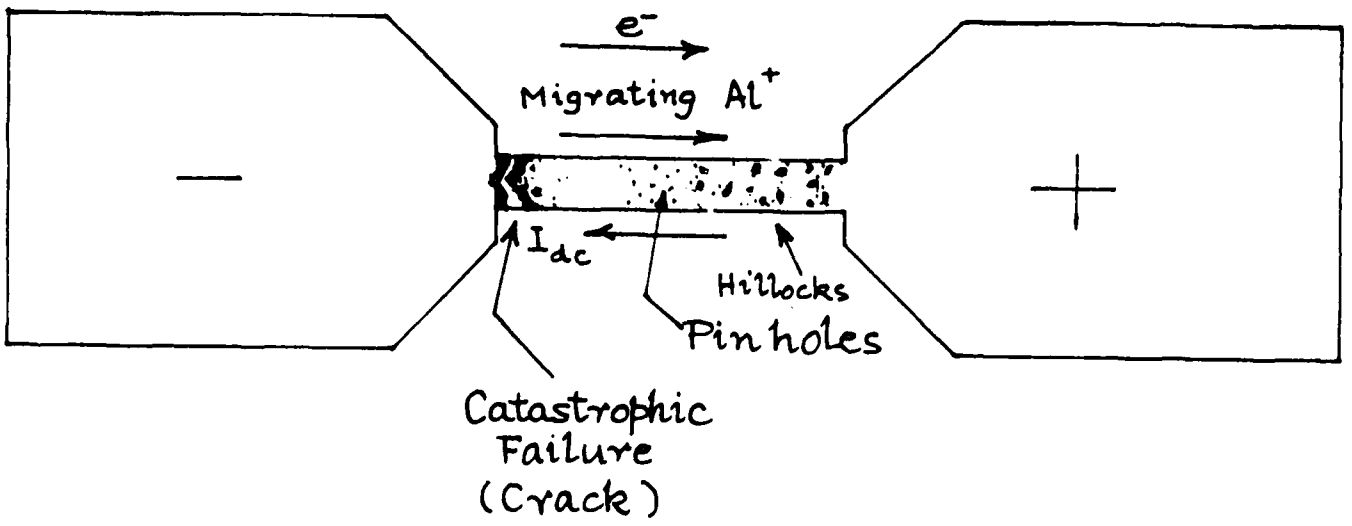

Fig. 5 Complete break of electrical conduction due to material migration

Repetition of the experiment on structures of other shape, i.e. with additional transitions from the conducting line to the bonding pads showed that pinholes or fine voids have also the tendences to nucleate at or near these transitions (Fig. 7).

These results are understandable as follows: The electron-wind associated voids (ultimately leading to a crack) near the cathode end are due to two reasons: (i) non-uniformity in the current density J near the part of the line where it opens up to the wider electrodes so that the rate, at which material is transported away in the direction of electron flow, is larger than the material supplied from the cathode electrode. This leads to a depletion of material, (ii) a positive temperature-gradient in the line near the cathode end due to Joule heat produced by the high current and with better cooling near the ends due to the wider electrodes.This temperature variation results in a difference in the ionic mobilities in this region leading to depletion of material in the form of voids. Hillocks formed on the line on the anode-side are due to accumulation of material in the negative temperature-gradient region there in the direction of electron-flow. The formation of pin-holes near the middle of the line are again due to a higher ionic mobility there due to a maximum in temperature profile there. The formation or appearance of voids near such transitions as those to the bonding pads or at discontinuities such as corners are then expected to be due to the discontinuities in the current density in these regions. A conclusion of these results is that the occurance of conductor-discontinuities,in fact any variation in the width along the metallization, should be avoided as far as possible so as to prevent the nucleation of voids. Providing efficient heat sinks is thus also expected to minimize the damage due to any temperature gradients.

In order to estabiish the activation energy associated with a current induced material migration, meantime to failure (MTF) measurements were performed on a number of identical samples with a line width of 13 µm, a thickness of 1050 Å and a length of 100 µm, identically current

stressed with J = 3 x 10^6 A/cm^2 at different temperatures in the range 20 - 120° C, using a constant current source and an x-t recorder. The results were then plotted ($\frac{1}{MTF}$ vs $^{1}/_{T}$), and from the resulting Arrhenius plot, expected to satisfy the relationship (within the statistical error-limits)

$$\frac{1}{MTF} = K^{*} A J^{n} \exp(-Eg/kT), \qquad \text{—— (2)}$$

an activation energy Eg of 0.40 eV was obtained which lies within the range of Eg (0.29 - 0.84) eV as reported by various workers [9-12]. A MTF technique is good for the qualitative study of the damage phenomenon, but an estimation of the basic value of Eg is erraneous by this technique owing to the very large J and higher strike temperature in the void region.

In order to avoid large-signal electron wind effects and to analyse electro transport in the early stages a resistance monitoring (RM) technique was then introduced which should lead to more accurate and reliable estimation of Eg. Four voltage probes along the length of the conducting line were incorporated to monitor the resistance of the different zones of the current-stressed line.

A new test structure, as shown in Fig. 3 was employed. The maximum increase of resistance was always observed for Zone I, as dented in Fig. 6, near cathode, where the convergence of current line produces the strongest voiding effect. Our technique of measurement followed the details as published by previous authors. [10] From the measured rate of increase of resistance $\frac{\Delta R}{\Delta t}$ (of Zone I) in the steady state of electro transport, one can measure the drift velocity v_β of the migrating Al-ions by the relation. [10, 13]

$$v_\beta = \beta \cdot \frac{1}{R_0} \cdot \frac{\Delta R}{\Delta t} \cdot l \qquad (3)$$

where l is the distance between the cathode and the voltage probe (length of zone I here),

R_0 is the equilibrium resistance of the segment or zone I (to include the increase in resistance due to Joule heating) just prior to steady electro tansport.

and β is a constant factor which depends on the ratio of the grain-size to the width of the stripe. For small grain size $\beta = 1.11 \simeq 1$.

AB : CURRENT ELECTRODES

EF
DE
CD } : VOLTAGE PROBES

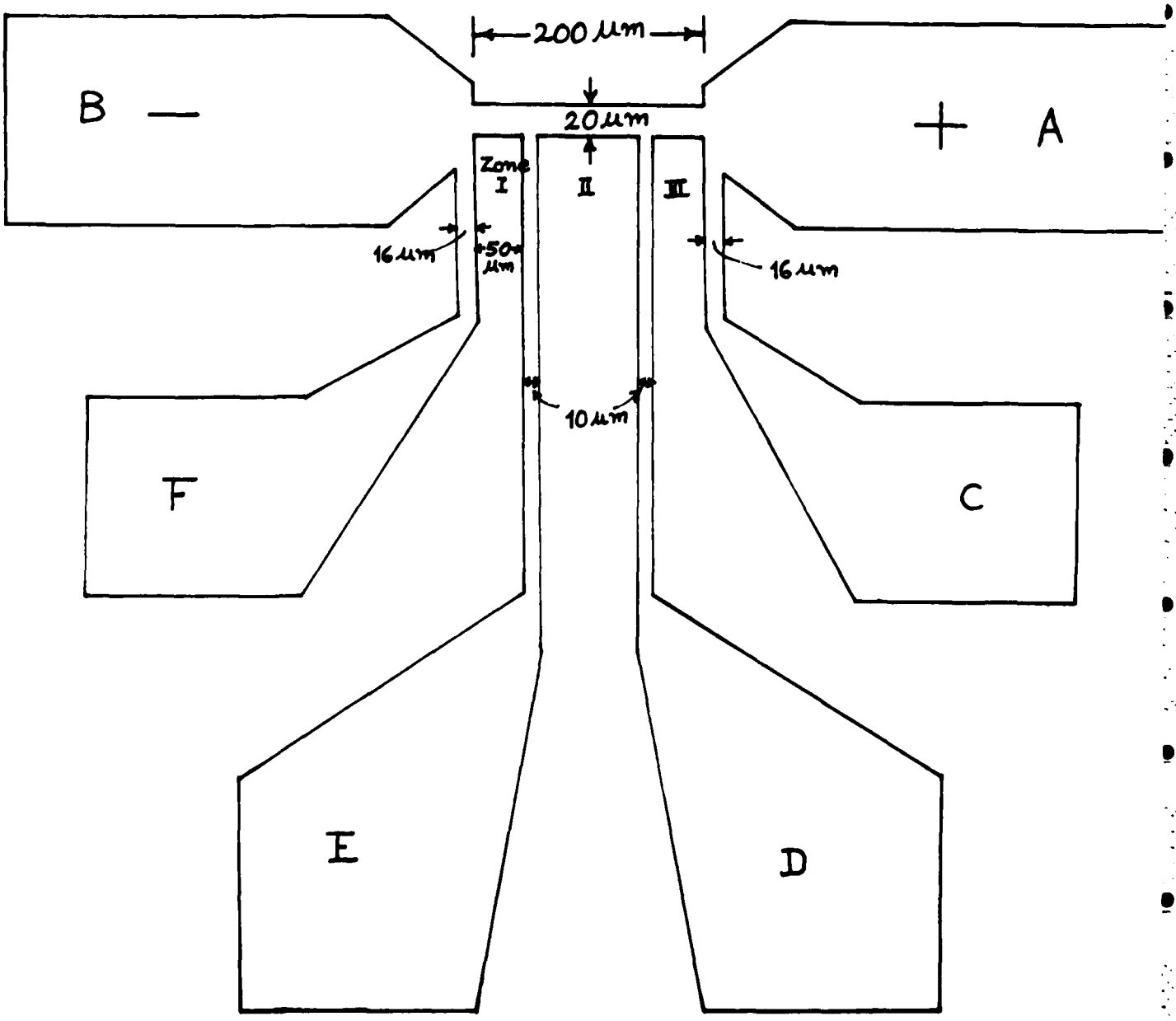

Fig.6 Experimental electrode structure for resistometric measurements

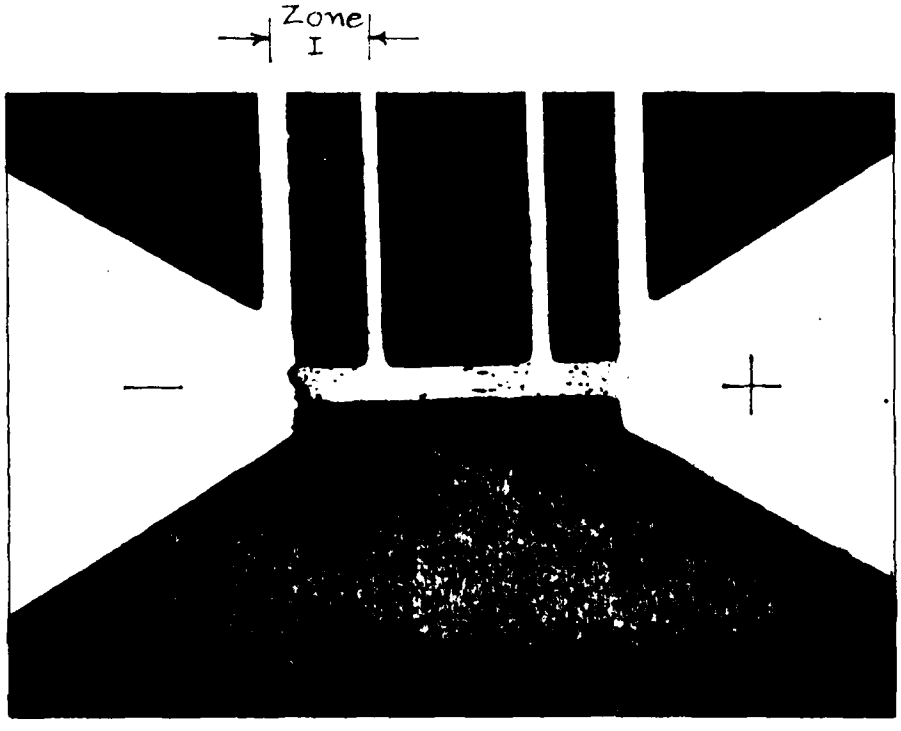

Fig. 7

Damage caused by'electron-wind' voiding in Al/Glass structure for $J = 2.5 \times 10^{6}$ A cm^{-2} at 50-100° C: Crack propagation across the entire cross-section near the cathode end, hillock formation near the anode end, and pin-holes or voids at and near the transitions to the bonding pads.

The activation energy Eg can then be estimated from the measured drift velocities v_β of the migrating Al-ions at different temperatures of the stripe (including any effect of Joule heating in connection with our strike-temperature estimation) by making use of equations (1a) - (1c).

Estimations of Eg and the constant K have been done from the measured temperature dependance of $\frac{v_\beta T}{J}$ which fits into the Arrhenius plot corresponding to Eg (1b) by using this RM technique for the following metallizations.

1. Al over corning glass (Al/Glass),
2. Al over semi-insulating (s.i.) GaAs (Al/GaAs),
3. Al over corning glass with an interfacial Cr-layer (Al/Cr/Glass) (1150 Å/350 Å : e-beam / normal evaporation)

and

4. Al over s.i.GaAs with an interfacial Cr-layer (Al/Cr/GaAs). (1070 Å/210 Å : with e-beam evaporation)

Al- and Al/Cr-metallizations were evaporated using identical photo-resist masks by the contact process under identical conditions of technological processes. The films were deposited in an evaporation chamber with a vacuum of 1×10^{-6} Torr. The width of the conducting line of the structures was 20 µm, its active length about 200 µm divided into three zones (as shown in Fig. 6) of lengths 50, 100 and 50 µm successively.

The thickness of the Al-films was about 1000 Å and that of the Cr-interface had a range of (200 - 350 Å). The rate of Cr-film deposition was about 1 Å/s, while that of the Al-film was about 4 Å/s up to the first 500 Å and then about 6 to 8 Å/s for the next 500 Å. Before the deposition, the surface of the glass-substrate was cleaned with Balzer's substrate cleaner solvent, while the GaAs wafer (which has a (100) oriented, polished surface as supplied by Sumitomo Electric Co., Japan) was cut into rectangular samples (size about 8 mm x 7 mm and and thickness 0.40 mm), the polished surfaces of which were cleaned in acetone at room temperature to remove possible organic

contaminants and crystal dust (spread on the surface in the process of cutting the samples from a large wafer). Each substrate-slice was examined before film deposition under the optical microscope. All this was done to ensure identical known conditions of substrate before metallization. After metallization, the samples were current-stressed for a current density $J = 1.8 \times 10^6$ A/cm^2. The type of electron-wind damage seen on such structures is shown in Fig. 7.

From the measured values of drift velocity v_β of migrating Al-ions, as determined from the measured rate of increase of resistance for the zone I of the strike at different temperatures, $\ln \frac{v_\beta T}{J}$ was plotted against $\frac{1}{T}$. The measured data was found to fit into linear curve, indicating that the Arrhenius diffusion law is being obeyed in electro transport. From the slope of the linear Arrhenius plots (in accordance with Eqn.(1b), the values of the activation energy Eg for the diffusion process in differenct Al-metallizations on various substrates were evaluated, along with the values of the constant K from the intercept which includes the diffusion coefficient D_o (at $T \to \infty$). The values of Eg and K taken together according to Eqns(1) give the value of drift velocity v_β of the migrating ions at any temperature for a particular value of current density J. This value of v_β reflects the damage to a current-stressed metallization due to electro transport or electro migration.

The values of the activation energy Eg, constant K and drift velocity v_β at 100^0 C for $J = 1.8 \times 10^6$ A/cm^2 obtained in Al-metallizations on Glass and GaAs are shown in Table 3, while those for Al-metallizations with an chromium interfacial layer are shown in Table 4.

The values of the activation energy E_A obtained indicate that the predominant diffusion mechanism in thin Al-films is grain boundary diffusion. The lower value of v_β in the metallization on GaAs (as compared to that on glass) suggests that the electro migration damage is slower for Al/GaAs structures than for Al/Glass.

TABLE 3

Parameters deciding the formation of voids, and material migration due to electro transport in Al-metallizations as relevant for gate metallizations in GaAs MeSFETs.

1. v_β - Drift velocity of migrating Al-ions at a particular temperature for a const. J
2. E_A - Activation Energy for electro migration for the involved diffusion process.
3. K - Constant = $\frac{D_0 \, Z^* \, e \, \rho}{k}$

in accordance with the equation

$$\frac{v\beta \, T}{J} = K \exp \left(- \frac{E_A}{k} \cdot \frac{1}{T} \right)$$

Structure	Substrate surface Treatment	Temperature Range	$\frac{v_\beta}{J}$ at 100^0 C for J= 1.8×10^6 A/cm^2 (cm/s)	E_A (eV)	K ($\frac{cm^3 \, K}{As}$)
Al/Glass	with Balzers' substrate cleaner solvent	$50 - 110^0$ C	3.1×10^{-8}	0.46	1×10^{-5}
Al/GaAs	Polished GaAs surface cleaned with acetone at room temperature	$60 - 140^0$ C	7.0×10^{-9}	0.61	3×10^{-4}
AL/GaAs	Polished GaAs surface 1.cleaned with organic solvents & then etched in alcaline etchant	$100 - 220^0$ C	1.9×10^{-10}	0.52	4×10^{-7}

TABLE 4

Parameters v_β, E_A and K deciding material migration due to electro tranpsort in Al-metallizations over a chromium-interface

Structure	Substrate surface treatment	Temperature Range	v_β at 100^oC for $J = 1.8 \times 10^6$ A/cm^2 (cm/s)	E_A (eV)	K ($\frac{cm^3 K}{A \cdot s}$)
Al/Cr/ Glass	with Balzers' substrate cleaner	25^o - 125^o C	1.1×10^7	0.37	4.0×10^{-6}
Al/Cr/ GaAs	polished GaAs surface cleaned with acetone at room temperature	20^o - 100^o C	7.9×10^{-9}	0.14	1.3×10^{-10}

The difference in the values of E_A for Al-metallizations (Table 3 & Table 4) on different substrates indicates that, under identical conditions of Al-evaporation, the values of Eg and the other electro transport parameters depend strongly on the type of the substrate and on the surface properties of the substrate. Since the substrate surface determines the grain-size and grain-structure of the films deposited on it, and since the size and structure of the grains in the metallization has been found to influcence strongly the grain-boundary diffusion, the electro migration damage is expected to be affected by the surface-quality of GaAs.

The higher value of E_A in Al/GaAs metallizations (o.61 ev), compared to that in Al/Glass, suggests that at ordinary temperatures, material migration is very low but at higher temperatures it is expected to increase rather rapidly.

The main aim of the present work is to establish the optimum conditions for surface treatment of GaAs and for evaporation of different aluminium Schottky metallizations on them to obtain stable MeSFET gate structures. If one deposits the Al-films under standard evaporation conditions and keep them identical for different substrates, one finds that electron-wind voiding or electro migration damage is lower in an Al/GaAs system than for Al/Glass. The desired criterion for low electro migration damage of devices are: the lowest possible value of drift velocity v_β of the migrating Al-ions at a particular temperatur (or in the temperature range of operation of the device) for a constant current density J; the highest possible value of Eg with a low value of the constant K.
In order to have more stable Al-gates in GaAs MeSFETs, the next stage of investigation is to deposit the Al-metallizations on GaAs (semi-insulating) with its polished surface treated with different technological processes such as with different chemical etchants.

The damage parameters related to material migration due to electro transport in Al/Cr metallizations, as obtained from the experimental Arrhenius plots, are shown in Table 4. The two different types of substrates tried are again glass and GaAs. The values of the activation energy E_A obtained are too low for grain boundary diffusion (particularly in Al/Cr/GaAs metallizations).

Ideal (oxide-free) surface diffusion, based on trapped holes or islands in the film (for which E_s = 0.28 eV [14]), may be a possibility for material migration, although also this is unlikely as it requires an adequate number of trapped holes or islands. The low value of the drift velocity v_β in Al/Cr/GaAs and the small value of K suggests that in Al/Cr metallizations on GaAs, the electro transport is very slow. Further, a very low value of activation energy E_A (= 0.14 ev) in this metallization suggests that the effect is also not so temperature sensitive, i.e. the damage due to electro migration is small at room temperature and it does not increase rapidly at higher temperatures. On the other hand the damage due to electro migration in Al/Cr-metallizations on glass is quite noticeable and is more temperature sensitive. At increased temperatures (above around 200° C), an additional and rather dominant failure mechanism seems to be an interaction or interdiffusion of Al and Cr, as observed in the relatively rapid burn out of these Al/Cr/Glass metallizations at higher current densities ($J \simeq 4 \times 10^6$ A/cm^2) Fig. 8a. When this Al/Cr metallization was current stressed with such a high current density, the large Jouly heating causes the film temperature to rise to above 200° C, and a quick burn out failure was observed within about 5 min. Fig. 8a, which has an Al-film as the top layer, showed not only a crack developed near the cathode electrode but also serious damage due to the composition of the active line particularly in the region of the positive temperature gradient where a wide portion of the Al-film turned brownish. This seems to be due to an interaction or interdiffusion of Chromium into Al. An examination of the Cr-side of the Al/Cr metallization (on Glass), Fig. 8b, showed the disappearance of the Cr-film (steel grey in colour) underneath the Al-layer (silvery shining layer) in the damaged region of the film, as mentioned in Fig. 8a. This observation suggests that the damage failure mechanism in an Al/Cr metallization on glass, at higher temperatures ($> 200^{\circ}$ C) can also be interdiffusion or interaction of Al and Cr. The conclusion is that the damage in Al/Cr-metallizations on glass is caused not only by electron wind voiding (i.e. electro transport) but also by interdiffusion of Al and Cr particularly at higher temperatures, while Al/Cr-metallizations on GaAs seem to be quite stable concerning any electro transport damage at the temperature ranges of interest and that this damage is also by temperature-sensivity.

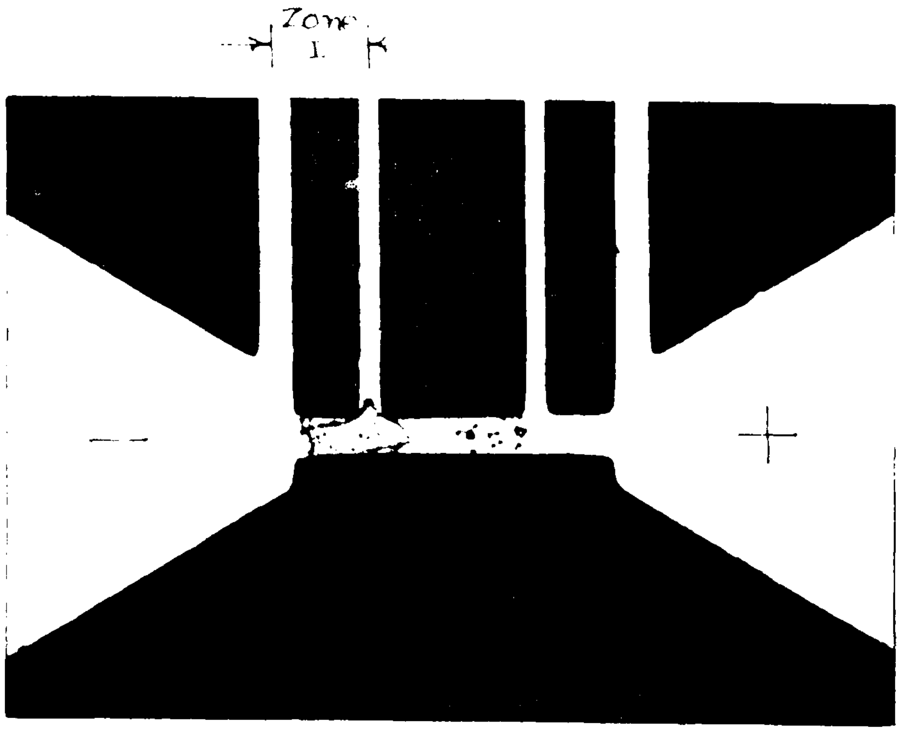

Fig. 8a

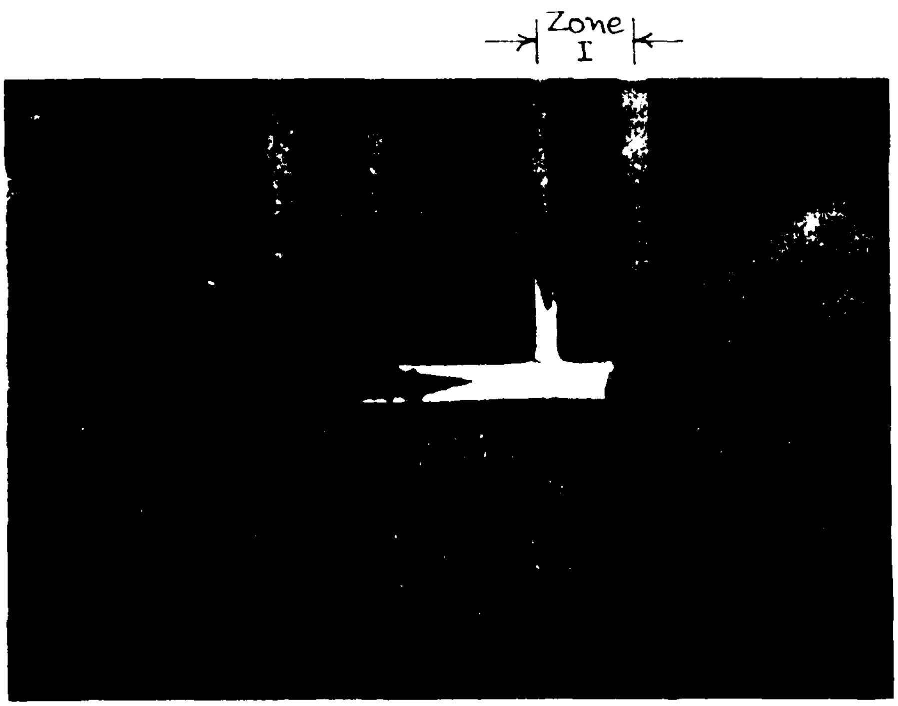

Fig. 8b

Figs. [illegible] rated [illegible]

a) [illegible]

b) [illegible] ode.

[illegible] and Cr

One of the important results obtained with different Al-metallizations is that electro migration damage depends on the nature of the substrate and on its surface quality. From the view-point of stability with the Al-gate structures in GaAs MeSFETs concerning electron-wind voiding, we have further examined the electro-transport damage parameters in dependance on the surface quality of the GaAs, as this could affect the grain size and structure of the Al-films deposited on it. The treatment of the GaAs surface, after chemical-polishing with organic solvents (like acetone, trichlor ethylene and methanol-nearly for 1o minutes in each) has been attempted with different chemical etchants (alkaline and/or acidic) before Al-deposition. The following etching solutions have been used on GaAs:

i. the pre-evaporation (alkaline) etchant consisting of NaOH (2 % by weight) + H_2O_2 (3o % conc. - 4 % by volume) mixed in the ratio 1:1. The etching was performed at 23^o C (room temp.) for 1 min. It has been established from ESCA surface analysis work done in our laboratory (and reported in the previous Chapter II of this Report) that this etchant removes undesired oxides of As and Ga from the GaAs surface to a large extent.

ii. the acidic etchant consisting of H_2SO_3 (conc.) + H_2O_2 (3o % conc.) + H_2O (deionized) mixed to the ratio of 1 : 1 : 1. The etching was performed at 23^o C (room temp.) for 1 min. ESCA surface analysis has shown (reported in Chapter II of this Report) that a GaAs surface chemically polished in organic solvents as detailed in (i) and then etched in this solution, is found to be rich in Arsenic Oxide.

After etching GaAs samples in these alkaline and acidic etchants examination of the surfaces under an optical microscope has revealed that the alkaline etchant (No.(i))leaves the GaAs surface quite shining and clear, while the acidic etchant produces a surface which is dull, bluish and quite often with fine straight scratch marks.

After fabricating bonding contacts to current and voltage electrodes with silver-epoxy the Al/GaAs structure based on a specific type of etching, was current stressed using a current density of $J = 1.83 \times 10^6$ A/cm^2

at room temperature. The resistance monitoring technique was used to measure the drift velocity v_β of the migrating ions. At room temperature, any effect due to material migration was found to be too small to be measured with any reliable accuracy within 24 hours of current stressing. The sample was then current stressed at elevated temperatures and, including the effect of Joule-heating, the rate of increase of resistance of Zone I of the metallization was measured in the temperature range from 1oo - 22o^0 C. The values of v_β were also determined, using Eqn (3). The measured data at different temperatures (i.e. ln $\frac{v_\beta T}{J}$ vs. 1/T) was found to fit again into a linear Arrhenius plot, from which the values of Eg and K were determined. These values and the drift velocity v_β of the migrating Al-ions at 1oo^0 C has also been shown in Table 3 (bottom row).

Let us examine these results keeping in mind that the desired properties of metallizations for low damage rates are a high value of Eg with a low value of the constant K or the lowest possible value of the drift velocity v_β at a particular temperature (say 1oo^0 C) for a constant value of J. The comparison of these parameters for Al-gate metallizations indicates that a GaAs surface, chemically polished and etched in a ($NaOH + H_2O_2$) etchant gives a value of v_β which is the lowest of the three systems shown, whereas the value of the grain-boundary-diffusion activation energy remains reasonably high (Eg = o.52 ev) and the constant K(i.e. 4 x 1o^{-7}) involving D_o remains very small.

This investigation, therefore, suggests that at temperatures below 1oo^0 C , the damage caused by electro migration is small in Al-metallizations evaporated on a GaAs surface, which is chemically polished and etched in a ($NaOH + H_2O_2$) etch solution.

The investigations on Al-gate-metallizations with GaAs surfaces treated with other etchants such as acidic ones as detailed in (ii) etc. are not yet satisfactorily completed and will be presented in the next report. It is also planned to correlate the observed facts interims of the grain-strucure of the GaAs surface and that of the resulting Al-metallization with the help of a scanning or transmission electron microscope.

Preliminary attempts for the surface photographs of the Al-metallizations on GaAs (semi-insulating) with a scanning electron microscope did rot lead to any information regarding the grain-structure due to the poor contrast of the image formed both by the scattered electrons as well as by the back-reflected e-beam owing to high resistivity of the substrate on which Al-metallizations are deposited. Attempts were then made to take the transmission electron microscope (TEM) photograph of the surface but this required a cantilever - type of suspended metal film with no GaAs underneath. Therefore, we tried to make use of a replica technique to take the surface impression on an organic solvent sprayed on to our Al/GaAs structure. This solvent hardens quickly on to the metallization and can be easily removed as replica containing the surface topography of the metallization. On this hardened organic layer, platinum and carbon layers are successively deposited. The impression of the surface are thus now transferred to the Pt/C film which is investigated for the TEM photograph. This investigation to correlate the observed electron-wind damage phenomenon with the grain-structure of the Al-metallization and that of GaAs surface structure is also being carried out.

It is also planned to carry out these investigations on Al-gate-metallizations with Titanium (Ti) interfacial layer i.e. on structures like Al/Ti/GaAs or Ti/Al/Ti/GaAs and then to correlate the stability of these gate-metallizations with the surface-structure of the metallizations and surface-treatments of GaAs - substrate.

CHAPTER IV

INTERDIFFUSION EFFECTS AT THE TRANSITION Al-GaAs

The results of our studies concerning field-assisted-interdiffusion effects at the Al-GaAs transition that had been presented in the last annual report, were entirely based on experiments undertaken at room temperature and under normal atmospheric conditions. This means, that the influence of oxygen, nitrogen and CO_2 on our results can not be neglected. Indeed we have observed large oxygen concentrations at the Al-GaAs interface which seem to be dependent on the electric field applied for long periods. Indiffusion of oxygen for example can of course be prevented by undertaking such experiments in oxygen free, inert gases or in a vacuum system. Therefore an apparatus was developed which enables us to carry out these long-time experiments simultaneously with several samples, both in vacuum as well as under various atmospheric conditions and different temperatures. Experimental efforts at elevated temperatures in connection with Arrhenius plots might probably enable us to estimate the activation energies of the various interdiffusion effects.

The preparation of the GaAs surfaces before metal evaporation constitutes another very important aspect concerning stability and interdiffusion properties of metal-GaAs contacts. Previous work has shown that the chemical composition of GaAs surfaces, that means the amount of oxidized Ga and As, absorbed oxygen etc., is strongly dependent on different methods of surface treatment used during GaAs device fabrication (see also part II of this report).

During this period of the work, our experimental efforts were concentrated on evaluating the influence of chemical treatment of the GaAs surface before metal evaporation on field assisted interdiffusion effects occuring at the metal-GaAs transition. We chose Al for metallization because it

represents one of the most widely used types of metallization in GaAs device fabrication. Fig. 9a shows the structure of the samples which consist of thin aluminium layers with well defined geometrical areas on semiinsulating GaAs. An accurate definition of the quality of the contact area that is to be analyzed by XPS, needs to be made to obtain reliable and reproducable results. Before metal evaporation all samples were subjected to a standard wet-organic cleaning process, consisting of successive rinsing in hote acetone, trichlorethylene and methanol for about five minutes in each solvent. Afterwards, three diferent types of sample sets were prepared by etching in $NaOH + H_2O_2 + H_2O$, $KOH + H_2O$ and $H_2SO_3 + H_2O_2 + H_2O$ respectively for one minute. (Fig. 9b).
The fabrication process was finished by the definition of the metal contacts using photolithography and liftoff-techniques.

For each experimental set three identical samples were fabricated (Fig. 9c). One serves as a reference sample whereas the other two are biased positively or negatively for about 2oo hours. The biasing voltage was 65 Volts. All experiments were carried out at room temperature (23^{o} C) and in a vacuum system ($1.1o^{-5}$ mbar) to avoid additional oxidation or in-diffusion of ambient gases during long time stressing. Before and after the biasing experiments the current-voltage characteristics of the samples were recorded. The concentration profiles of the Al-layer and the Al-GaAs interface were obtained by XPS sputter profiling of both, the reference sample and the positively and negatively biased samples after finishing the long time stressing experiments. Their profiles have been computed from Al $2_{p\ 3/2}$, O $1_{s\ 1/2}$, As $2_{p\ 3/2}$ and Ga $2_{p\ 3/2}$ lines. For the determination of the concentration profile of oxidized aluminium, the energy shift of the Al $2_{p\ 3/2}$ ox. line due to the formation of an aluminium oxide was of course taken into account.
Comparing the corresponding experimental results, several important conclusions can be made.

1) Fig. 1oa and Fig. 1ob show the profiles of the aluminium and the aluminium oxide concentration of samples etched in sodium hydroxide and potassium hydroxide respectively before metal evaporation. One can

EXPERIMENTAL PROCEDURE

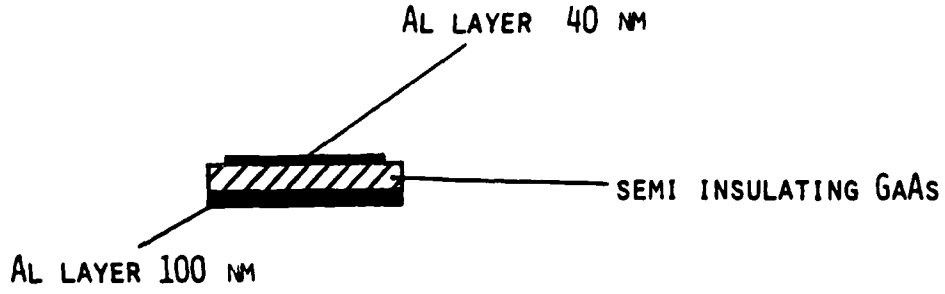

A) SAMPLE STRUCTURE (CROSS-SECTION)

1) NaOH (2 % WEIGHT): H_2O_2 (30 %) (4 VOL %)
1 : 1

2) KOH : H_2O
5 : 1

3) H_2SO_3 (CONC.) : H_2O_2 (30 %) : H_2O
1 : 10 : 10

B) PRE-EVAPORATION ETCHANTS USED

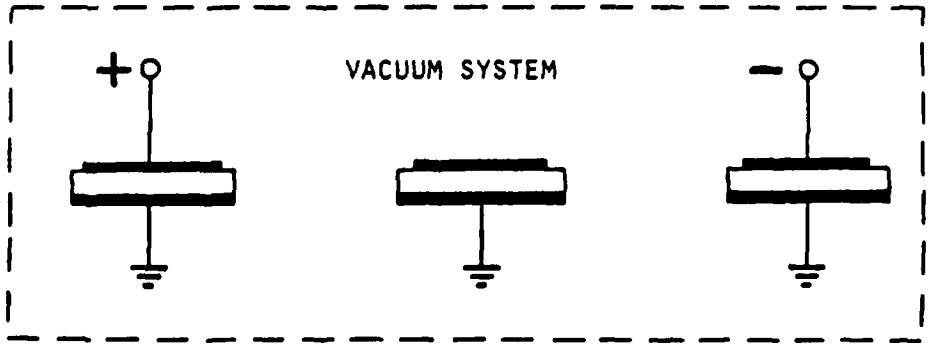

C) BIASING THE SAMPLE SETUP IN A VACUUM SYSTEM

Fig. 9

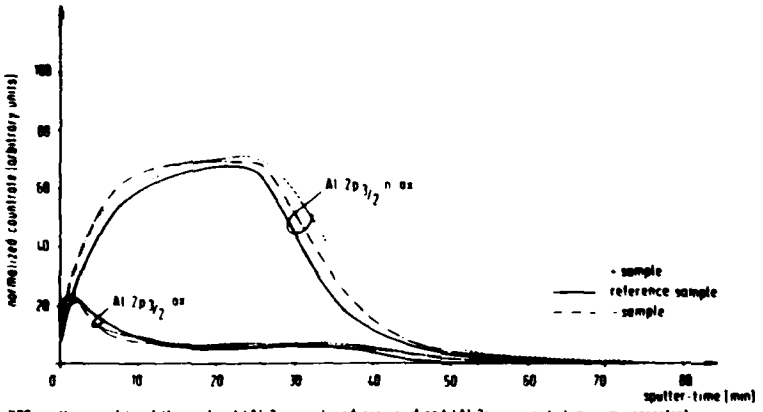

XPS sputter - profile of the oxidized (Al $2p_{3/2}$ ox) and non - oxidized (Al $2p_{3/2}$ n ox) aluminium concentration

a) Pre - evaporation etchant $KOH - H_2O$

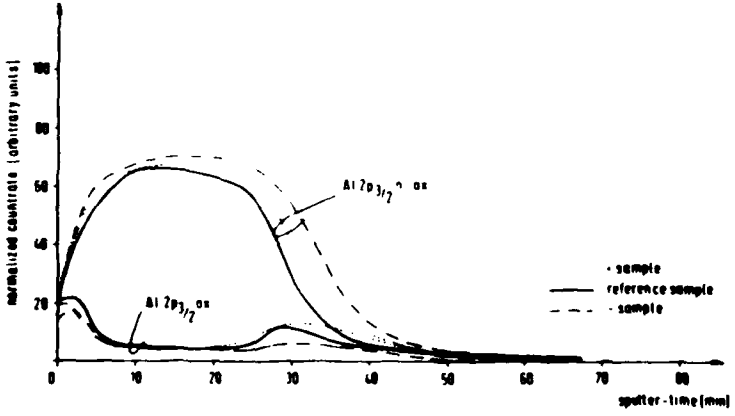

XPS sputter - profile of the oxidized (Al $2p_{3/2}$ ox) and non - oxidized (Al $2p_{3/2}$ n ox) aluminium concentration

b) Pre - evaporation etchant $Na_2B_4O_7 - H_2O_2 - H_2O$

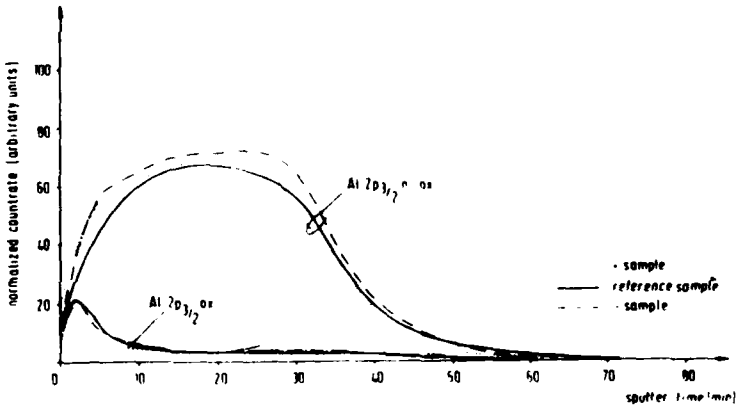

XPS sputter - profile of the oxidized (Al $2p_{3/2}$ ox) and non - oxidized (Al $2p_{3/2}$ n ox) aluminium concentration

c) Pre - evaporation etchant $H_2SO_3 - H_2O_2 - H_2O$

Fig. 1o

generally observe a broadening of the aluminium concentration profile for both sample sets, irrespectively whether the samples had been biased positively or negatively during long time-stressing. This behaviour confirms our observation we have presented in the last annual report. It is possible that this effect is caused by a field-assisted diffusion of aluminium across and along grain boundaries so that grain boundary removal or restructuring is taking place and a reduced sputter rate can therefore be observed. This explanation might be supported by the observation that the amount of broadening depends on the GaAs surface treatment before metal evaporation. Samples etched in sulfurous acid before evaporation for example show practically no Al-concentration-profile broadening (Fig. 1o c) in comparison to samples etched in sodium hydroxide or potassium hydroxide (Fig. 1o a,b). It seems reasonable to assume that the observed effects depend on the structure of the Al-layer because different etchants of course yield different surface properties on GaAs which may then result in different nucleation and growth processes during metal evaporation and therefore change the microscopic structure of the metal film |15| . Since the activation energy for diffusion along grain boundaries is smaller than for intra-grain diffusion |16|, diffusion effects at room temperature are strongly affected by the grain structure and the number of grain boundaries and therefore by the film structure itself.

2) Another very interesting effect occuring during bias stressing can be observed by considering the amount of oxygen at the interface before and after sample stressing (Fig. 11-13). It is apparent that positive bias causes an increase in oxygen concentration at the interface whereas negative biasing nearly maintains the oxygen concentration or even causes a depletion of oxygen in the case of samples that had been etched in sodium hydroxide before Al evaporation (Fig. 11). A systematic analysis of the XPS spectra reveals that oxygen at the interface is entirely bonded to aluminium. No galliumoxide or arsenic oxide could be detected. This means that a reduction of the native oxides on the GaAs surface had taken place during aluminium evaporation. It is interesting that the aluminiumoxide at the interface seems to have another

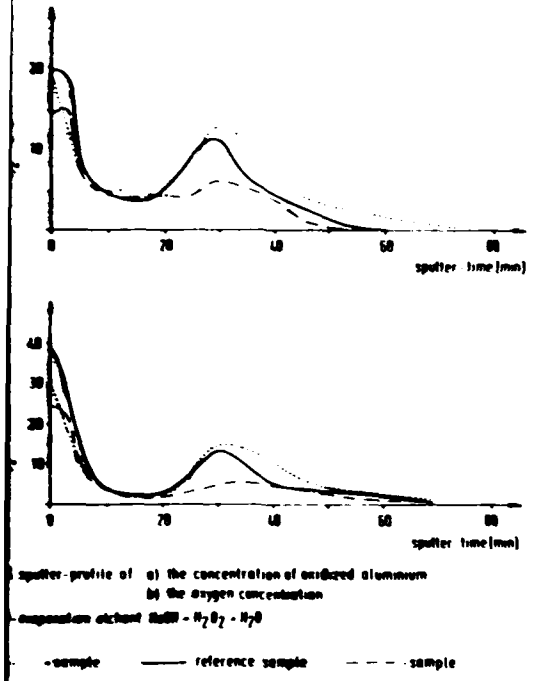

Fig. 11

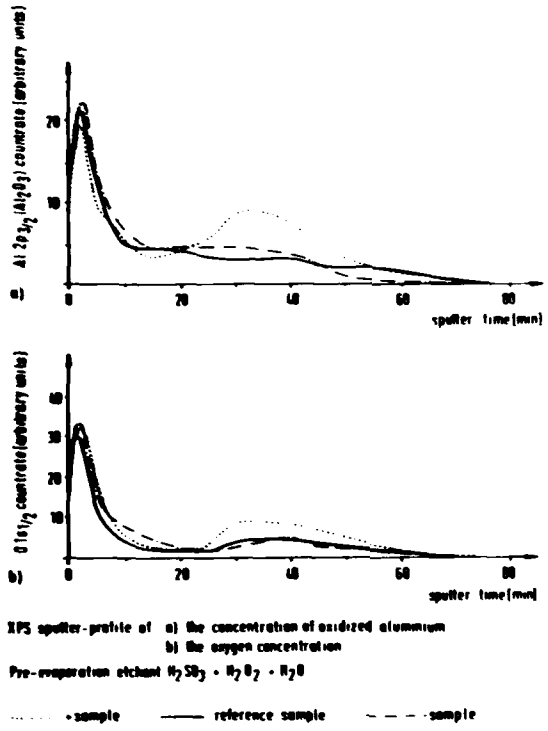

Fig. 12

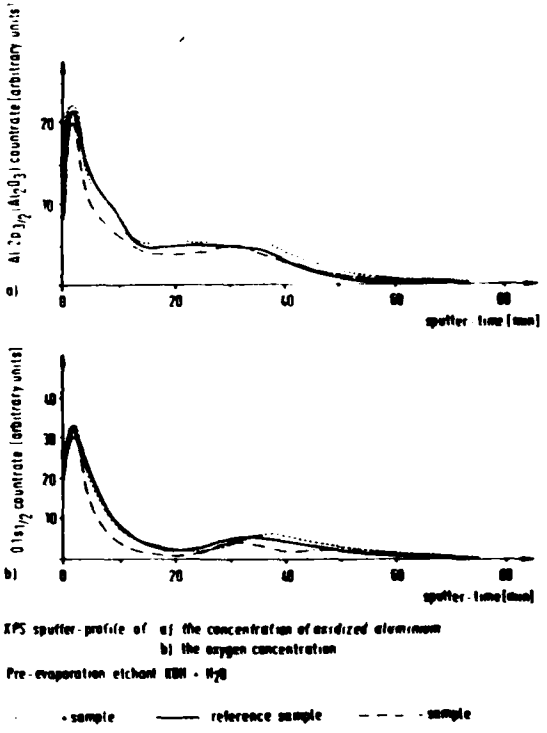

Fig. 13

chemical composition than the Al-oxide in free Al surfaces. This is indicated by the Al $2p_{3/2}$ spectral lines for aluminium surface oxides and interface oxides (energy difference about o.6 eV). It should be mentioned that an increase in aluminiumoxide concentration at the interface after positive biasing has been observed in all sample sets, independent on the type of pre-evaporation etchant which had been used. Both, the initial oxygen concentration at the interface and the oxygen accumulation after positive biasing are found to be directly affected by the GaAs surface preparation before Al metallization. This is in agreement with results obtained previously at the Institute that different etchants applied on GaAs surfaces change both type and concentration of native surface oxides (see also part II of this report). Using potassium hydroxide as pre-evaporation etchant for example (Fig. 13) only a small initial oxygen concentration at the interface and only small changes of this concentration could be observed after biasing in contrast to the two other etchants used for sample preparation. It is interesting that these changes in oxygen concentration at the interface occur even when the biasing experiments are undertaken in a vacuum system. Since no indiffusion from the ambient is possible in this case, the oxygen accumulation at the interface can probably be considered as a field-assisted redistribution of oxygen or aluminiumoxide which is available at the interface or in the grainboundaries of the Al-layer. This redistribution process can possibly be explained to be a defect mechanism in connection with negatively changed vacancies in the grain boundaries of the Al-layer or at the interface.These negatively changed vacancies may then be able to move against the direction of the electric field by changing their places with neighbouring neutral atoms. More investigations in this field have still to be undertaken in the future to explain the proper physical mechanism of these rather complicated and complex effects.

3) Fig. 14 show the Ga $2p_{3/2}$ ratio at the interface for different sample treatments and biasing conditions. These diagramms have been computed from the XPS spectra taking into account the shift of the gallium and arsenic concentration profiles that is due to the aluminium-concentration-profile broadening mentioned above. It is apparent that the Ga to As ratio generally decreases immediately at the interface for all samples independent of the preevaporation etchant used and the polarity of the bias during long time stressing. An analysis of the XPS spectra reveals that the decrease of the Ga to As ratio seems to be due to an arsenic accumulation at the interface. The magnitude of this accumulation is influenced by both the chemical surface treatment before metal evaporation and the biasing condition during the stresssing experiments. Comparing Fig. 14 a, b, c and Fig. 11 - 13 yields a strongcorrelation between the oxygen concentration and the Ga to As ratio at the interface. Positive biasing for example increases the oxygen concentration and the Ga to As ratio at the interface simultaneously. Nevertheless an arsenic overshoot at the interface can still be observed. We don't know exactly at the moment whether this increase of the Ga to As ratio after positive biasing is due to field assisted outdiffusion of arsenic or an indiffusion of Ga atoms. Further experiments will have to be undertaken, especially improved depth resolutions and different kinetic energies of the sputtering Ar ions during profiling to clarify these effects and to exclude any sputter related troubles like preferential sputtering and a decrease of depth resolution with increasing sputter depth.|17|

4) As mentioned above, current-voltage characteristics of the samples were monitored before and after bias stressing. Typical shapes of the I-V characteristics obtained will be explained in connection with Fig. 15 which shows the positive and negative part of the I-V characteristic of a sample treated with potassium hydroxide before aluminium evaporation. A relatively steep current increase can be observed at low voltages (region I) followed by a region showing very high differential resistances (II) and finally a region (III) with a very steep increase of current at high voltages.

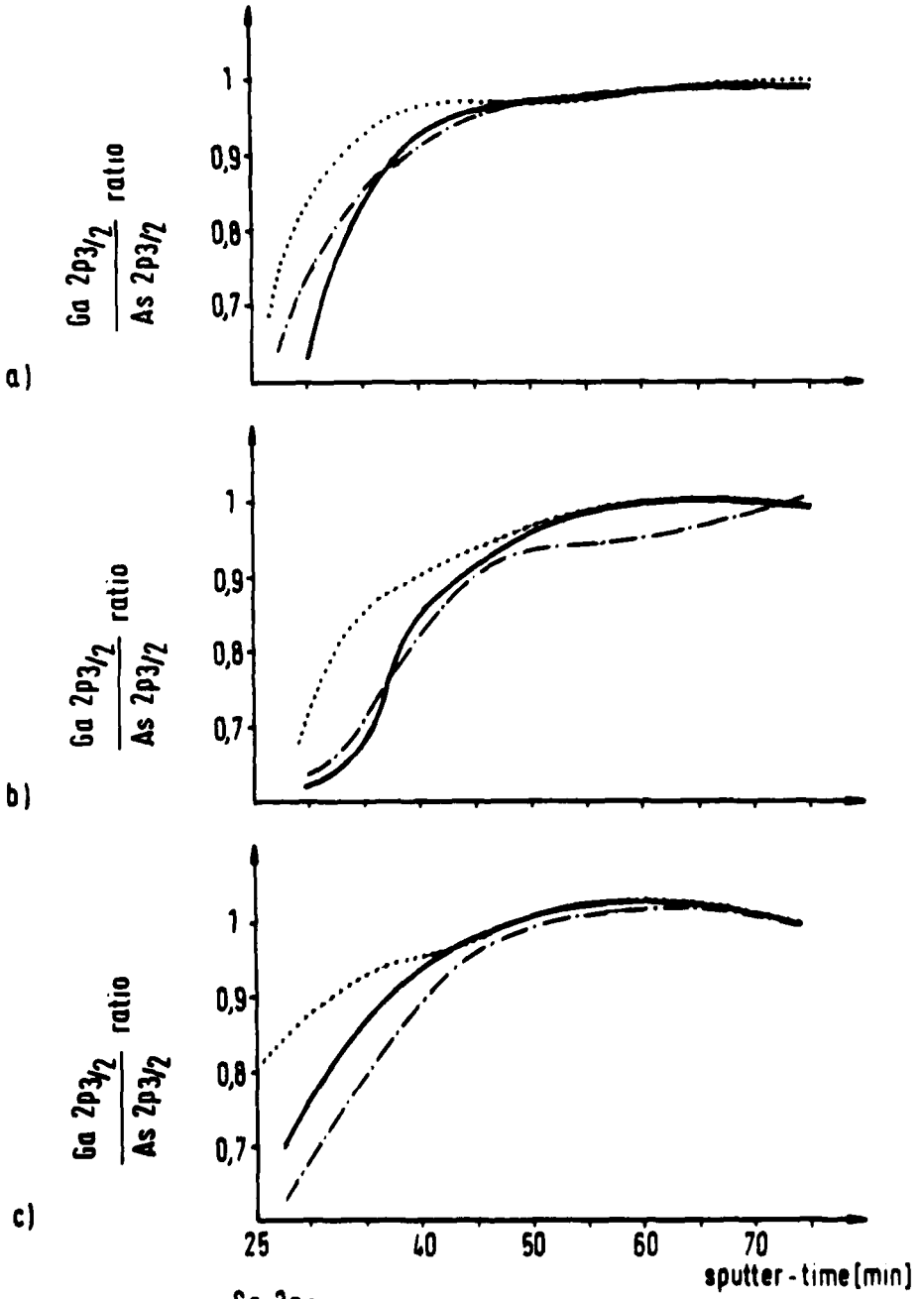

Change of the $\frac{Ga\ 2p_{3/2}}{As\ 2p_{3/2}}$ ratio after biasing the samples

Pre-evaporation etchants: a) $KOH + H_2O$

b) $H_2SO_3 + H_2O_2 + H_2O$

c) $NaOH + H_2O_2 + H_2O$

..... + sample —— ref. sample —·—·— - sample

Fig. 14

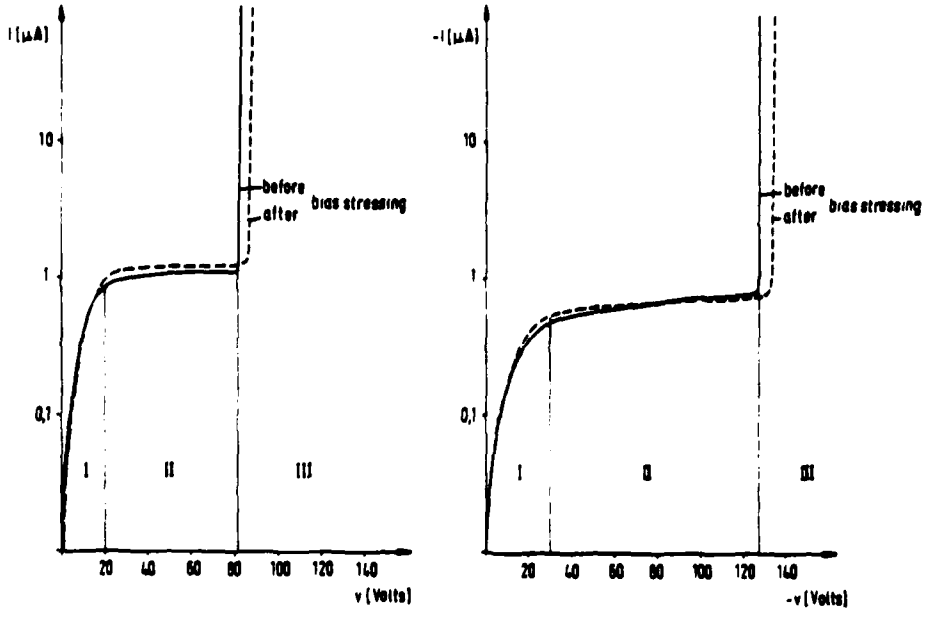

Current-voltage characteristic: Preevaporation etchant: KOH + H_2O
positively bias-stressed

Fig. 15

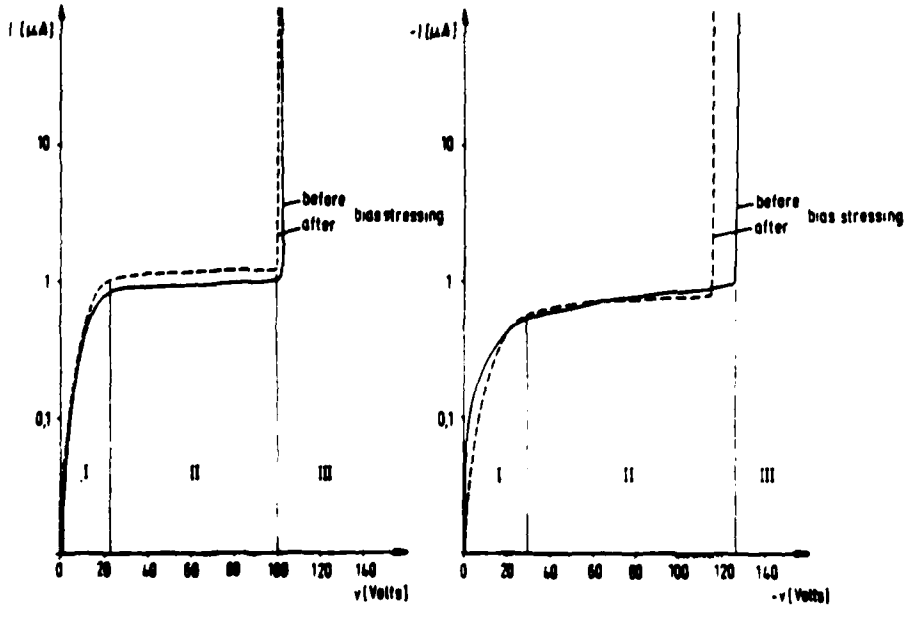

Current-voltage characteristic: Preevaporation etchant KOH + H_2O
negatively bias-stressed

Fig. 16

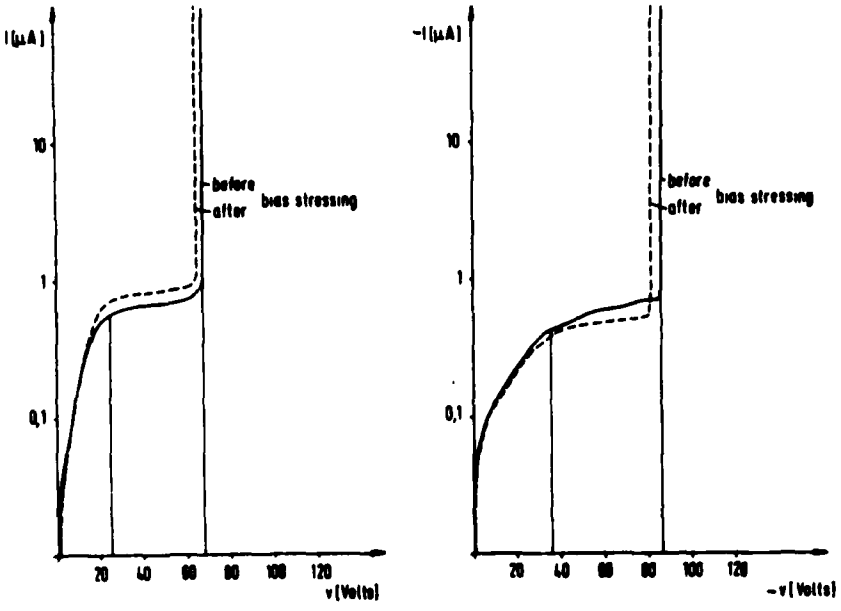

Current-voltage characteristic: Preevaporation etchant:

$H_2SO_3 + H_2O_2 + H_2O$

positively bias-stressed

Fig. 17

According to Kao |18| this current voltage characteristics seems to be typical for double injection in solids between two similar Schottky contacts (Al-GaAs-Al). The band structure of an Al-GaAs Schottky contact shows that in this case the Schottky barrier for electrons is higher than for holes (o,8 eV for electrons in comparison to o.65 eV for holes) |19|. Therefore at low voltages a hole-current flow from the anode to the cathode of a Al-GaAs-As contact system seems to be more likely than an electron flow in the opposite direction. The current is said to be bulk limited in that region (I). In region II of the current-voltage characteristics, no further additional holes can be extracted from the anode in spite of increasing electric fields with increasing voltage between the contacts. The current flow is contact limited in that region. The steep current increase in region III indicates the beginning of double injection. That means that now electrons are injected at the cathode and both electrons and holes contribute to the current flow. The positive and negative parts of the I-V characterstics show a rather asymmetrical behaviour especially with regard to the transition from the contact-limited area tothe region of double injection. This asymmetry is possibly the result of the different surface roughness of the back- and the frontside contacts of the samples (The wafers used for sample preparation have had an unpolished backside and a polished frontside). Increased surface roughness of course leads to locally increased electric fields just underneath the contact, which results in a premature onset of double injection if the backside contact serves as a cathode so that electrons can be injected(for the positive region of the current-voltage characteristic).This means generally that the treshold voltage for double injection is strongly dependent on the contact structure. Moreover Kao |18| has shown that the saturation current at the treshold voltage between regions I and II of the I-V characteristic is a function of the barrier height for the injected carriers (possibly holes in that case). Therefore changes of electronic states at the Al-GaAs interface can probably affect the shape of the I-V characteristic.

Indeed we observed a strong dependence of the measured I-V characteristics on both the surface treatment of the samples before metallization and on longtime stressing experiments (Fig. 15-17). Samples etched in sulfurous

acid, for example, show much lower treshold voltages for the beginning of double injection than samples etched in potassium hydroxide(Fig. 17). After sample stressing the following changes of the I-V characteristic coulo be found

- An increase of the plateau-current in the current limited region was observed, both in the positive and in the negative part of the I-V characteristics. However, this change is more pronounced in the positive part. It is most likely that this is due to the asymmetric contact system. In the positive region of the I-V characteristic the current in the contact limited region is governed by the Al-GaAs contact on the polished side of the samples whereas the current saturation in the negative part can be referred to the unpolished, less ideal Al-GaAs backside contact. Therefore, the saturation current in the positive part of the I-V characteristics seems to reflect the properties of that contact system that will have been XPS analysed lateron. At the moment it is not possible to determine definitely, whether the saturation current is affected by the polarity of the bias-stressing experiments since the differences measured so far are within the experimental errors. A series of statistical measurements will have to be undertaken to obtain a reliable understanding.

- The treshold voltage for the onset of double injection has also changed after bias stressing. Since this treshold is determined by the beginning of electron injection from the cathode, the negative part of the I-V characteristics reflects the properties of the corresponding contact system in this case. It seems that the treshold voltage is dependent on the polarity of bias stressing. Considering samples etched in potassium hydroxide e.g. , one can observe an increase in treshold voltage after positive biasing (from 126 to 132 Volts) and a decrease after negative biasing (from 126 to 115 Volts) (Fig. 15, 16). Nevertheless more experiments will have to be undertaken to eliminate stray effects.

The bias stress dependence of the I-V characteristics might be reduced firmly to field assisted structural changes in the Al-layer (see also point 1) and secondly to electronic states at the Al-GaAs interface that have been changed

by one of the diffusion mechanisms detected by XPS sputter profiling, because changes in the electronic state density at the interface will affect the barrier height and therefore the I-V characteristics, too. Table 5 gives a short summary of our results obtained so far. Here, the most important details are summarized shortly and assigned to both, the GaAs surface treatment before aluminium evaporation and the biasing conditions during long-time stressing.

For future work it is planned firstly to complete our measurements on the contact system aluminium-semi-insulating GaAs as mentioned above and secondly to extend our investigations on different Schottky and Ohmic contacts on n-and p-GaAs.

Table 5

Summary of the results

Surface treatment before Al-metallization	$NaOH + H_2O_2 + H_2O$		$KOH + H_2O$		$H_2SO_3 + H_2O_2 + H_2O$	
Surface structure after etching	slightly rough surface		smooth surface		rough surface	
Biasing conditions	positive	negative	positive	negative	positive	negative
Aluminium-concentration-profile broadening	yes	yes	yes	yes	not very much pronounced	not very much pronounced
Change of oxygen concentration at the interface	accumulation	depletion	accumulation	nearly const.	accumulation	nearly constant
Change of the Ga/As ratio	increase	decrease	increase	nearly const.	increase	nearly constant
Saturation current positive I-V characteristic)	--	--	increase	increase	increase	increase
Saturation current (negative I-V characteristic)	--	--	nearly const.	nearly const.	increase	decrease
Treshold voltage, double inj. (pos. I-V characteristic)	--	--	increase	decrease	decrease	increase
Treshold voltage, double inj. (neg. I-V characteristic)	--	--	increase	decrease	decrease	decrease

A P P E N D I X

List of Student Projects related to the Present Report

1. El-Hage, Hussein
   Soebandi, Anang - St 1219 - 14.1o.1982
   Herstellung und Untersuchung der elektrischen Eigenschaften von Metall-Halbleiterübergängen
   (Manufacture and characterization of metal-semiconductor contacts)

2. Diakopouloi, Danai - D 1227 -
   Herstellung und Untersuchung von Chrom-Kontakten auf GaAs
   (Manufacture and characterization of Cr-contacts on GaAs)

3. Krizek, Franz - D 1251 - 2. 3.1983
   Optische Bestimmung der Barrierenhöhe von Schottky Dioden auf unterschiedlich geätzten GaAs-Oberflächen
   (Optical Determination of barrier height of Schottky contacts on differently etched GaAs surfaces)

4. Grigoriadis, Nikolaos - D 13o3 - 27. 2.1984
   Untersuchung der Spannungsfestigkeit eng benachbarter Elektroden für monolithisch integrierte HF-Schaltkreise
   (Voltage stability of closeley spaced electrodes for monolitic GaAs IC's)

5. Charzakas, Athanase - D 13o8 - 12. 3.1984
   Experimentelle Untersuchung des Verhaltens unterschiedlich gestalteter Metall-Halbleiter-Übergänge bei hohen elektrischen Feldstärken
   (Experiments on differently shaped metal-semiconductor transitions regarding high electric voltages)

6. Scholz, Rainer - D 1315 - 4. 7.1984
   Einfluß der Oberflächenbehandlung von GaAs auf die Spannungsfestigkeit monolithisch integrierter HF-Schaltkreise
   (Influence of surface treatment on GaAs on voltage stability of monolitic GaAs IC's)

7. Reinhard, Hans Walter - D 1335 - 19. 9.1984
   Entwurf und Aufbau eines steuerbaren, geregelten Schaltnetzteils für hohe Ausgangsspannungen bis 1000 Volt
   (Studies concerning a stabilized power supply with voltages up to 1000 V)

8. Ladas, Panagiotis
   Maros, Konstadinos - St 1344 -
   Herstellung und Untersuchung von Metall-Halbleiterkontakten für GaAs-Höchstfrequenztransistoren
   (Manufacture and Characterization of special metal-contacts for GaAs transistors)

9. Pitz, Gerhard - D 1347 - 12. 2.1985
   Herstellung planarer Strukturen für GaAs-Höchstfrequenzbauelemente und experimentelle Untersuchung ihrer Zuverlässigkeit
   (Planar structuring für GaAs devices concerning high-reliability behaviour)

10. Dworschak, Peter - D 1355 -
    Softwareentwicklung für ein 6502-Mikroprozessorsystem zum Aufbau eines adaptiven, programmierbaren Temperaturereglers
    (Software-development for a 6502 microprocessor system for a programmable temperature controller)

R E F E R E N C E S

[1] J. M. Dumas, J. Paugam, C. Le Mouellic, J. Y. Boulaire:
"Long Term Degradation of GaAs Power MeSFET's Induced by Surface Effects"
21th Annual Proc. Reliability Physics, 1983, pp 226-228

[2] J. G. Tenedorio, P. A. Terzian
"Effects of Si_3N_4, SiO and Polyamide Surface Passivations on GaAs MeSFET Amplifier RF Stability"
IEEE Electron. Device Lett., 1984, Vol 5, pp 199 - 2o2

[3] W. Mönch:
"Electronic Characterization of Compound Semiconductor Surfaces and Interfaces"
Thin Solid Filmx, 1983, Vol. 1o4, pp 285-299

[4] G. P. Schwartz, G.J. Gualtieri, G.W. Kammlott, B. Schwartz:
"An X-Ray Photoelectron Spectroscopy Study of Native Oxides on GaAs"
J. Electrochem. Soc., 1979, Vol. 126, pp 1737-1749

[5] C.D. Thurmond, G.P. Schwartz, G.W. Kammlott, B. Schwartz:
"GaAs Oxidation and the Ga-As-O Equilibrium Phase Diagramm"
J. Electrochem. Soc.,198o, Vol. 127, pp 1366-1371

[6] Irie, T., Nagasako I., Kohzu H. and Sekido K.,
Trans. Microwave Theory & Techniques,
Vol. MTT-24, pp 321-328 (1976).

[7] Katsukawa K., Kose Y., Kanamoric M. and Sando S.,
IEEE Proc. Reliability Phys., Vol. 21st, pp 59-62 (1984).

[8] Blech, I.A.
J. Appl. Phys., Vol. 47, pp 12o3 - 12o8 (1976).
Blech, I.A. and Kinsbron,
Thin Solid Films, Vol. 25, pp. 327-334 (1975).

9 Black, J.R.
- Proc. 3rd Int. Congr. on Microelectr., Munich (1968)
- IEEE Trans. Electron Devices, Vol. ED-16, 338 (1969).
- Proc. IEEE, Vol. 57, 1589 (1969).

|10| Hummel R.E., de Hoff R.T. and Geier H.J.,
J. Phys. Chem. Solids, Vol. 37, pp 73-8o, (1976).

|11| Attardo, M. J. and Rosenberg, R.
J. Appl. Phys., Vol. 41, 2381 (197o).

|12| Sim, S.P.,
Microelectron. Reliab., Vol. 19, 2o7 (1979)

|13| Rodbell K. P. and Shatynski,
Thin Solid Films, Vol. 1o8, pp. 95-1o2 (1983).

|14| Schreiber H.-U.,
Solid State Electronics, Vol. 24, pp. 583-589 (1981)

|15| K.L. Chopra,
Thin Film phenomena
McGraw-Hill Book Company (1969), pp 137-254

|16| M.-A. Nicolet
"Diffusion Barriers in thin Films"
Thin Solid Films, 1978, Vol. 52, pp. 415-443

|17| M.P. Seah, M.E. Jones
Roughness Contributions to Resolution in Ion Sputter
Depth Profiles of Polycrystalline Metal Films
Thin Solid Films, 1984, Vol. 115, pp. 2o3-216

|18| K.C. Kao
Double Injection in Solids with non-ohmic contacts
I. Solids without defects
J. Phys. D: Appl. Phys., 1984, Vol. 17, pp 1433-1448

[19] S.M. Sze
Physics of Semiconductor Devices
2nd edition, John Wiley & Sons (1981), pp. 245-312

END

FILMED

6-85

DTIC